A type IV translocated Legionella cysteine phytase counteracts intracellular growth restriction by phytate

Weber, Stephen ; Stirnimann, Christian U ; Wieser, Mara ; Frey, Daniel ; Meier, Roger ; Engelhardt, Sabrina ; Li, Xiaodan ; Capitani, Guido ; Kammerer, Richard A ; Hilbi, Hubert

Abstract: The causative agent of Legionnaires' pneumonia, Legionella pneumophila, colonizes diverse environmental niches, including biofilms, plant material, and protozoa. In these habitats, myo-inositol hexakisphosphate (phytate) is prevalent and used as a phosphate storage compound or as a siderophore. L. pneumophila replicates in protozoa and mammalian phagocytes within a unique "Legionella-containing vacuole." The bacteria govern host cell interactions through the Icm/Dot type IV secretion system (T4SS) and 300 different "effector" proteins. Here we characterize a hitherto unrecognized Icm/Dot substrate, LppA, as a phytate phosphatase (phytase). Phytase activity of recombinant LppA required catalytically essential cysteine (Cys(231)) and arginine (Arg(237)) residues. The structure of LppA at 1.4 Å resolution revealed a mainly -helical globular protein stabilized by four antiparallel -sheets that binds two phosphate moieties. The phosphates localize to a P-loop active site characteristic of dual specificity phosphatases or to a non-catalytic site, respectively. Phytate reversibly abolished growth of L. pneumophila in broth, and growth inhibition was relieved by overproduction of LppA or by metal ion titration. L. pneumophila lacking lppA replicated less efficiently in phytate-loaded Acanthamoeba castellanii or Dictyostelium discoideum, and the intracellular growth defect was complemented by the phytase gene. These findings identify the chelator phytate as an intracellular bacteriostatic component of cell-autonomous host immunity and reveal a T4SS-translocated L. pneumophila phytase that counteracts intracellular bacterial growth restriction by phytate. Thus, bacterial phytases might represent therapeutic targets to combat intracellular pathogens.

DOI: https://doi.org/10.1074/jbc.M114.592568

JBC Papers in Press. Published on October 22, 2014 as Manuscript M114.592568
The latest version is at http://www.jbc.org/cgi/doi/10.1074/jbc.M114.592568

A type IV-translocated *Legionella* cysteine phytase counteracts intracellular growth restriction by phytate*

Stephen Weber[1], Christian U. Stirnimann[2,#], Mara Wieser[2], Daniel Frey[2], Roger Meier[3], Sabrina Engelhardt[4], Xiaodan Li[2], Guido Capitani[2], Richard A. Kammerer[2] & Hubert Hilbi[1, 5*]

From the [1] Max von Pettenkofer Institute, Department of Medicine, Ludwig-Maximilians University Munich, 80336 Munich, Germany

[2] Paul Scherrer Institute, Department of Biomolecular Research, 5232 Villingen, Switzerland

[3] Scientific Center for Optical and Electron Microscopy, ETH Zurich, 8093 Zurich, Switzerland

[4] Institute of Veterinary Physiology & Zurich Center for Integrative Human Physiology (ZIHP), Vetsuisse Faculty, University of Zurich, 8057 Zurich, Switzerland

[5] Institute of Medical Microbiology, Department of Medicine, University of Zurich, 8006 Zurich, Switzerland

[#] Current address: Biomedical Automation Technologies, Otto-Stern-Weg 7, ETH Zurich, Zurich, Switzerland

*Running title: Type IV-translocated *Legionella* phytase

To whom correspondence should be addressed: Hubert Hilbi, Institute of Medical Microbiology, Department of Medicine, University of Zurich, 8006 Zurich, Switzerland. Tel.: +41 (0)44 634 2650, Fax: +41 (0)44 634 4906; E-mail: hilbi@imm.uzh.ch

Key words: bacterial effector protein, *Dictyostelium*, host-pathogen interactions, Icm/Dot, *Legionella*, *myo*-inositol hexakisphosphate, pathogen vacuole, phosphoinositide, phytate, type IV secretion

Background: *Legionella* governs pathogen-host interactions by translocating ~300 „effector" proteins through a type IV secretion system.
Results: The hitherto unrecognized effector LppA is a phytase that counteracts intracellular bacterial growth restriction by phytate.
Conclusions: The chelator phytate is a bacterio-static component of cell-autonomous immunity, which is degraded by a bacterial effector.
Significance: *Legionella* LppA represents the first translocated phytase and a potential therapeutic target.

ABSTRACT

The causative agent of Legionnaires' pneumonia, *Legionella pneumophila*, colonizes diverse environmental niches including biofilms, plant material and protozoa. In these habitats, *myo*-inositol hexakisphosphate (phytate) is prevalent and used as a phosphate storage compound or as a siderophore. *L. pneumophila* replicates in protozoa and mammalian phagocytes within a unique "*Legionella*-containing vacuole" (LCV). The bacteria govern host cell interactions through the Icm/Dot type IV secretion system (T4SS) and ~300 different "effector" proteins. Here we characterize a hitherto unrecognized Icm/Dot substrate, LppA, as a phytate phosphatase (phytase). Phytase activity of recombinant LppA required catalytically essential cysteine (Cys231) and arginine (Arg237) residues. The structure of LppA at 1.4 Å resolution revealed a mainly α-helical globular protein stabilized by four antiparallel β-sheets that binds two phosphate moieties. The phosphates localize to a P-loop active site characteristic of dual specificity phosphatases or to a non-catalytic site, respectively. Phytate reversibly abolished growth of *L. pneumophila* in broth, and growth

inhibition was relieved by overproduction of LppA or by metal ion titration. *L. pneumophila* lacking *lppA* replicated less efficiently in phytate-loaded *Acanthamoeba castellanii* or *Dictyostelium discoideum*, and the intracellular growth defect was complemented by the phytase gene. These findings identify the chelator phytate as an intracellular bacteriostatic component of cell-autonomous host immunity and reveal a T4SS-translocated *L. pneumophila* phytase that counteracts intracellular bacterial growth restriction by phytate. Thus, bacterial phytases might represent therapeutic targets to combat intracellular pathogens.

Legionella spp. are ubiquitous environmental bacteria that colonize diverse environmental niches including biofilms, plant material and protozoa (1-4). In free-living amoebae and mammalian phagocytes, *L. pneumophila* replicates within a "*Legionella*-containing vacuole" (LCV), employing the Icm/Dot type IV secretion system (T4SS) and ~300 different "effector" proteins (5-7). Some *L. pneumophila* Icm/Dot substrates target and subvert pivotal regulators of eukaryotic signal transduction and vesicle trafficking, such as small GTPases (8-13) or phosphoinositide (PI) lipids (14-16). Several *Legionella* effectors anchor to the LCV membrane by specifically binding to the phosphorylated phosphatidylinositol (PtdIns) headgroup of PI lipids, namely PtdIns(4)*P* (17-22) or PtdIns(3)*P* (23-25), which are implicated in secretory or endosomal vesicle trafficking, respectively. Moreover, *L. pneumophila* produces two non-homologous Icm/Dot-translocated PI 3-phosphatases, SidF and SidP, which might modulate the LCV PI pattern (26,27). SidF localizes to the LCV membrane and hydrolyses *in vitro* the phagosomal/endosomal PIs PtdIns(3,4)P_2 and PtdIns(3,4,5)P_3, possibly yielding PtdIns(4)*P* on LCVs directly or through the activity of the host PI 5-phosphatase OCRL1 (23). SidP hydrolyses *in vitro* the endosomal PI lipids PtdIns(3)*P* and PtdIns(3,5)P_2, thereby possibly contributing to the evasion of the endocytic pathway by the LCV. By virtue of their phosphorylated inositol head groups, PIs bear high resemblance to phytate (*myo*-inositol hexakisphosphate) and lower inositol phosphates.

Phytate is used as the major phosphorus storage compound by plants and is the most abundant organic phosphorus compound in the environment (28-30). Protozoa also synthesize phytate, and in particular the social soil amoeba *Dictyostelium discoideum* produces the compound in millimolar quantities (31-33). Phytate is rather inert; yet, phosphorus mineralization is catalyzed in a step-wise manner by specific phosphohydrolases (phytases), which are produced by a wide range of bacteria (29). The plant pathogen *Xanthomonas oryzae* uses a secreted phytase as a virulence factor for growth on phytate as the sole phosphate source (34). In addition to serving as a source of phosphorus, carbon and energy, phytate may also play a role in bacterial iron acquisition by chelating metal ions. Accordingly, *Pseudomonas aeruginosa* employs phytate as an iron siderophore (35,36). Phytate is also a prominent anti-nutrient able to complex several metal ion micro-nutrients, thus restricting their bioavailability (37).

Based on their sequence similarities, phytases are classified as four different groups comprising histidine acid phosphatases, purple acid phosphatases, β-propeller phosphatases or cysteine phytases (29,38,39). The conserved amino acid motif "CX_5R" is a hallmark of the "P-loop" (phosphate-binding) catalytic site of the prototypic cysteine phytase PhyA in *Selenomonas ruminantium* (39), as well as of eukaryotic and prokaryotic PI phosphatases such as PTEN (phosphatase and tensin homologue deleted on chromosome 10), *L. pneumophila* SidF and SidP (26,27,40), dual specificity Ser/Thr and Tyr protein phosphatases (DSP) (41), or the triple specificity DSP/PI phosphatase MptpB from *Mycobacterium tuberculosis* (42,43).

By using the phosphatase consensus sequence HCxxGxxRT as a search motif, we identified a *L. pneumophila* cysteine phytase. The phytase, termed LppA, hydrolyzes phytate and PIs *in vitro* and is translocated by the Icm/Dot T4SS into host cells, where it counteracts intracellular bacterial growth restriction by the chelator phytate.

EXPERIMENTAL PROCEDURES

Bacteria, cells and growth conditions – *L. pneumophila* strains (Table 1) were grown for 3 d on charcoal yeast extract (CYE) agar plates buffered with N-(2-acetamido)-2-aminoethane-sulfonic acid (ACES). Liquid cultures were inoculated in AYE medium at an OD_{600} of 0.1 and grown at 37°C to an OD_{600} of 3.0 – 3.4 (approx. 21-22 h) (17). Chloramphenicol (Cam) was added at 5 µg/ml to select for pMMB207-C-derived plasmids. Murine RAW 264.7 macrophages were

cultivated in RPMI 1640 medium supplemented with 10% FCS and 2 mM L-glutamine. *Acanthamoeba castellanii* (ATCC 30234) and *Dictyostelium discoideum* amoebae were propagated as described (44).

Chromosomal deletion of lppA, plasmid construction and site-directed mutagenesis - All plasmids used are listed in Table 1. DNA manipulations were performed according to standard protocols, and plasmids were isolated using kits from Qiagen or Macherey-Nagel. All PCR fragments were sequenced.

The chromosomal deletion of *lppA* was performed by double homologous recombination as described (44): 500 bp downstream and upstream fragments were amplified by PCR using the primer pairs oRM1/oRM2 and oRM3/oRM4, respectively (Table 2). Both fragments were inserted by a four way ligation into a pGEM-T-easy vector with a kanamycin resistance (Kan^R) cassette in-between using *Bam*HI sites and adenosine overhangs, yielding plasmid pRM2. Clones were analyzed by restriction digestion and sequencing. The Kan^R cassette flanked by upstream and downstream fragments was transferred into the pLAW344 suicide plasmid using *Not*I, yielding plasmid pRM3. *L. pneumophila* JR32 was transformed by electroporation with pRM3 and selected for Kan^R and Suc^S colonies. Positive clones were tested by PCR using the primer pairs oRM7/oKan3' and oRM8/oKan3'.

Translational CyaA- and M45-fusion proteins of *lppA* were constructed by PCR amplification of the corresponding DNA. The fragments were cut with appropriate restriction enzymes and inserted into pSH97, pMMB207-C-RBS-M45, or pMMB207-C-RBS-*gfp*-RBS, using the oligos oCR161/oCR162 or oRM5/oRM6, yielding plasmids pSH108, pRM1 and pWS31, respectively. Translational GST-fusion proteins of *lppA* were constructed as above with the exception that the first 16 amino acids of the LppA protein were deleted by PCR amplification of the *lppA* template. The *lppA* fragment was cloned into pGEX-6P-1 using the oligos oRM13 and oRM6, yielding plasmid pRM9.

The *S. ruminantium* phytase gene *phyA* (39) was synthesized by GenScript USA Inc. and delivered in commercial vector pUC57-Kan with flanking *Bam*HI and *Sal*I restriction sites. In the design, the intrinsic *Sal*I site of the gene was removed by a silent single base substitution maintaining the original amino acid sequence. The *phyA* gene was cloned with *Bam*HI and *Sal*I into pGEX-6P-1, yielding pWS25.

Site-directed mutagenesis of the P-loop residues C215A, K219A, G220D or R221A of $lppA_{\Delta 1\text{-}16}$ was performed with the QuikChange Lightning Multi Site-Directed Mutagenesis Kit (Agilent Technologies) according to the manufacturer's instructions. PCR amplification was carried out using primers carrying the corresponding point mutations to yield the plasmids pSE7 to pSE10. The methylated template pRM9 was digested with *Dpn*I.

Vector pAK7 was constructed by PCR amplification of the complementary primers pAK7fo/pAK7re, followed by restriction digestion with *Bam*HI/*Bsp*HI, and insertion into pET-28a(+) cut with *Bam*HI/*Nco*I (compatible with *Bsp*HI). The plasmid pWS11 was cloned by *Bam*HI/*Sal*I insertion of the PCR product of oWS25 and oWS26 into pAK7.

Phosphate release and protein-lipid overlay assay - GST fusion proteins were purified as previously described (25). Phytate (phytic acid sodium salt hydrate) was obtained from Sigma-Aldrich, and synthetic di-octyl PI and inositol phosphates were purchased from Echelon Biosciences Inc (Salt Lake City, USA). Phosphate release from phytate or PI substrates was assayed by a malachite green assay (Protein Tyrosine Phosphatase (PTP) Assay Kit, Sigma-Aldrich) in a total volume of 50 µl/well in a 384-well plate (Greiner) at 25°C. Substrates were prepared in 25 µl assay buffer (100 mM Tris-HCl, 120 mM NaCl, pH 7.4). To initiate the reaction, 25 µl of enzyme solution in assay buffer (0.05 – 5 µg protein) was added and mixed 3 times rapidly without blowing out. 25 µl of the malachite green acidic dye and vanadate ion complex (mixed 100:1 at least 30 min before use) were added to terminate reactions. The color was developed for 20 min, and absorbance was measured at 620 nm with a FLUOstar plate reader (BMG Labtech). All values for a series were standardized against the zero reading (enzyme solution and malachite green mixed, followed by addition of substrate solution), and 2-4 samples were used for each time point. A standard reference curve for phosphate release was generated using the 1 mM phosphate standard supplied with the kit.

The products of LppA from various PI lipids were assessed with PIP-strips (Echelon Biosciences Inc) treated with 0.5 µg/ml LppA for 10 min. Membranes were washed three times for 10 min with PBS. Subsequent binding of GST-$SidC_{P4C}$ or GST-LpnE probes and anti GST Western blots were carried out as previously described (17,18). Peroxidase-labelled secondary antibodies were visualized by ECL (Amersham).

Detection of LppA by Western blot - 30 ml AYE cultures of *L. pneumophila* wild-type, Δ*lppA* or wild-type harboring vector pRM1 were grown overnight at 37°C to early stationary phase. Cultures were standardized to an OD_{600} of 3.0 with AYE and pelleted at 12'000 × *g* for 15 min. Supernatants were decanted to new tubes and centrifuged again; this was repeated once. 5 ml of cell-free supernatants of each strain were loaded with a dot blot apparatus onto a nitrocellulose membrane under vacuum suction. The bacterial pellets were suspended in 30 ml Tris-buffered saline (TBS), and a 1.5 ml aliquot of each was boiled for 10 min at 95°C. Cell debris was pelleted, and 500 µl of lysate for each strain was loaded onto a nitrocellulose membrane under vacuum suction. The membrane was blocked for 1 h in TBS 4% milk powder and stained for 1 h with an affinity-purified polyclonal anti-LppA antibody (1:500; GenScript), followed by an anti-rabbit HRPO-tagged antibody (1:5'000) for 30 min.

Protein purification and crystallization - To produce $LppA_{21-314}$ for crystallization, plasmid pWS11 was transformed into chemically competent *E. coli* NiCo[DE3] (New England Biolabs) and plated on LB-Kan agar-plates containing 50 ug/ml Kan. Several colonies were picked, transferred into 100 ml LB medium containing 50 ug/ml Kan and incubated overnight at 37°C in an orbital shaker. 4 l of ZYM5052-Kan autoinduction medium (for protein production by auto-induction in high-density shaking cultures (45)) containing 50 ug/ml Kan were inoculated with 25 ml (1:40) of the overnight culture and grown at 37°C for 7 h in a large orbital shaker. The temperature was subsequently lowered to 20°C, and incubation was continued overnight. The cells were harvested by centrifugation at 5'000 rpm. Cell pellets were suspended in 100 ml lysis buffer (50 mM Tris pH 7.5, 500 mM NaCl, 10 mM imidazole, 10 mM β-mercapthoethanol (β-ME), 1 protease inhibitor cocktail tablet (Complete EDTA free, Roche Diagnostics)) and lysed on ice using three 1 min 100% amplitude sonication pulses (Vibra Cell sonication device (Sonics) equipped with a large preparative sonication tip). Soluble proteins were separated from cell debris by centrifugation (25'000 × *g*, 30 min), followed by filtration of the supernatant (0.45 µm).

Recombinant LppA was purified by immobilized metal affinity chromatography, followed by size-exclusion chromatography, using an ÄKTA Xpress chromatography machine. The supernatant was loaded onto a 5 ml HisTrap crude FF column. The column was washed with 20 CV (column volumes) of wash buffer 1 (50 mM Tris pH 7.5, 500 mM NaCl, 10 mM imidazole, 10 mM β-ME) and 20 CV wash buffer 2 (50 mM Tris pH 7.5, 500 mM NaCl, 60 mM imidazole, 10 mM β-ME). Recombinant LppA was eluted with 5 CV of elution buffer (50 mM Tris pH 7.5, 500 mM NaCl, 500 mM imidazole, 10 mM β-ME). The eluted protein was injected to a 26/60 HiLoad Superdex200 size exclusion column (SEC buffer: 50 mM Tris pH 7.5, 500 mM NaCl, 500 mM imidazole, 10 mM β-ME). The total yield was 155 mg of pure LppA. The protein was concentrated to 5 mg/ml using a 10 kDa-MWCO ultrafiltration concentrator (Millipore) and used for crystallization trials.

Crystallization experiments were carried out at the crystallization facility of the Swiss Light Source (SLS). Crystals were obtained with the sitting drop vapor diffusion method at 293 K, using a well solution containing 40 mM KH_2PO_4, pH 4.1, 16% PEG 8000 and 20% glycerol. Drops consisted of 1 µl protein solution and 1 µl well solution.

Data collection and structure determination - Diffraction data from a single LppA crystal were collected at 100 K on a PILATUS6M pixel detector at the SLS beamline X10SA using an X-ray wavelength of 1.0000 Å. The data was processed using XDS to a resolution of 1.4 Å. The structure was solved by molecular replacement and auto-rebuilt using PHENIX: four molecules per asymmetric unit were found using the monomeric structure of protein tyrosine phosphatase-like phytase from *Mitsuokella multacida* (PDB code 3F41) as a search model. Refinement and manual model rebuilding were carried out with PHENIX and Coot, respectively. The model was validated using MolProbity; analysis with EPPIC did not find any biologically relevant interfaces in the crystal lattice. Data collection and refinement statistics are shown in Table 3.

Translocation assay - To determine translocation of LppA, adenylate cyclase fusion proteins were generated and used to quantify the production of cAMP in the host cell as described (46). Briefly, RAW 264.7 macrophages were seeded at 5×10^5/ml into 96-well plates in a final volume of 100 µl/well and incubated at 37°C overnight. The macrophages were infected (MOI 50) with *L. pneumophila* wild-type or Δ*icmT* harboring plasmid pSH108 grown for 21 h in AYE supplemented with 0.5 mM IPTG. After 30 min of infection, cells were washed with PBS and lysed with 200 µl sterile water for 10 min. Lysis was enhanced by shaking the plate on a microplate shaker. Intracellular cAMP was measured by using the cAMP Biotrak enzyme immuno assay system (Amersham Pharmacia).

Extracellular growth assays - *L. pneumophila* wild-type was inoculated with an OD_{600} of 0.1 in 200 µL AYE in 96-well plate format. Three wells were used per sample per test condition. After 12 h growth at 37°C and 600 rpm on a temperature-controlled plate shaker (Eppendorf), 10 mM phytate was added for 6 h to one growth set. After an additional 6 h, the bacteria were pelleted for 10 min at 1000 × *g* and carefully suspended in fresh 37°C AYE medium. Growth on the plate shaker proceeded for another 12 h. OD_{600} measurements were taken with a FLUOstar plate reader and subtracted from input values.

Alternatively, *L. pneumophila* wild-type, Δ*lppA* mutant or wild-type harboring pRM1 (M45-LppA) were inoculated with an OD_{600} of 0.1 in 200 µL AYE in 96-well plate format. Three wells were used per sample per test condition (0 - 5 mM phytate). Unused wells were filled with 200 µl sterile water. Cultures were incubated on a temperature-controlled plate shaker at 24°C and 600 rpm. Growth was measured after 5 days (OD_{600}). Wild-type *L. pneumophila* was also grown in 3 mL AYE cultures at 37°C. Micro-nutrient supplementation was carried out with $FeN_3O_9 \times 9H_2O$ (Sigma-Aldrich), $ZnCl_2$ (Fluka), $CaCl_2$ (Fluka) or $MgCl_2 \times 6H_2O$ (Fluka). Phytate (final concentration 10 mM) was added to cultures at a ratio of 1:1 with each micro-nutrient. Cultures were inoculated in triplicate at an OD_{600} of 0.1 and allowed to grow for 21 h.

Intracellular growth assays and fluorescence microscopy - Intracellular growth assays under phytate load were performed with *A. castellanii* or *D. discoideum* amoebae cultured with increasing concentrations of phytate. The compound was added at 2.5 mM and the concentration was increased every two days until the cells were maintained in 10 or 5 mM phytate for *A. castellanii* or *D. discoideum*, respectively. *L. pneumophila* wild-type, Δ*icmT*, Δ*lppA* harboring pNT28 (GFP), or Δ*lppA* harboring pWS31 (GFP, LppA) were inoculated in AYE with Cam (5 µg/ml) and IPTG (1 mM), and grown to early stationary phase. *A. castellanii* or *D. discoideum* were seeded 5×10^4/well in 200 µl LoFlo (ForMedium) in a 96-well plate and allowed to adhere for 1 h. Each measured time point of the experiment required one 96-well plate with three allocated wells per strain. *L. pneumophila* cultures were diluted in LoFlo to 2.5×10^4/ml. Medium was removed from adhered cells and replaced with 200 µl of *L. pneumophila* dilutions. Plates were centrifuged at 1'000 × *g* for 5 min and incubated at 37°C for *A. castellanii* or 23°C for *D. discoideum*. As an input control, 20 µl of a 1:100 dilution of each strain used for infection was plated onto CYE agar, and colonies were counted after 3 d incubation at 37°C.

After centrifugation, one plate for *A. castellanii* (t = 0) was imaged by confocal microscopy using a Nikon Eclipse TE300 microscope with a Perkin Elmer UltraVIEW spinning disk system and a Hamamatsu Orca Flash 4.0 C-MOS camera. A Nikon 20× Plan Fluor objective was used in combination with filters 488 – 10BP/525 – 50BP and bright field. Image evaluation was carried out with Velocity 6.0.1 software (Perkin Elmer). Confocal images of the GFP channel and bright field were captured for each time point.

Quantitative plating assays were performed to complement microscope images, since GFP expression could vary between strains. To this end, the infected cells were lysed after microscopic imaging at a given time point, and bacterial dilutions were plated onto CYE agar following the method previously described for colony counting (47). *D. discoideum* amoebae were lysed and plated without imaging. CFU counts for *L. pneumophila* growth in cells not cultured under phytate load followed the same procedure in absence of phytate supplementation.

Competitive growth in *A. castellanii* between wild-type and *lppA* deletion strains was performed as described (47). Finally, the observation of PtdIns(4)*P* in *D. discoideum* by GFP-$SidC_{P4C}$ was carried out as previously described (21).

Statistical methods - Differences between *L. pneumophila* strains were evaluated by two-tailed unpaired Student's *t*-test assuming unequal variances. Statistical error of the mean is presented as +/- one standard deviation with 95% confidence intervals.

RESULTS

The type-IV translocated cysteine phosphatase LppA hydrolyses phytate and PIs in vitro - A PSI-BLAST search using the phosphatase consensus sequence HCxxGxxRT identified in the genome of *L. pneumophila* strain Philadelphia-1 (txid: 272624) a predicted 36.3 kDa protein, Lpg2819, annotated as a putative protein tyrosine phosphatase II of the DSP superfamily. The only other protein thus identified is annotated as a lysophospholipid acyltransferase. The same search with generic *L. pneumophila* (txid: 446) yielded results for "protein tyrosine phosphatase" in all sequenced strains. Finally, a search of all available genomes of the family Legionellaceae (taxid: 118969) yielded a hit for at least 9 different *Legionella* spp. Lpg2819 is conserved with shared synteny among all *L. pneumophila* strains sequenced thus far (including Philadelphia-1, Paris, Lens, Corby, Alcoy, 130b/AA100, Lorraine), as well as in *L. longbeachae* (64% identity), *L. shakespearei* (64% identity), and *L. dumoffii* (62% identity).

A closer bioinformatic inspection of Lpg2819 revealed an overall similarity to cysteine phytases of *Clostridium* (39% identity), *Stigmatella* (36% identity), *Pseudomonas* (34% identity) and *Xanthomonas* spp. (32% identity), as well as to PhyA from *S. ruminantium* (30% identity) (29,39,48) (Fig. 1A). The P-loop consensus sequence of *Legionella* spp. is strictly conserved in the phytases from *Clostridium acetobutylicum* and *Stigmatella aurantiaca*. Based on these similarities and the catalytic activities of recombinant Lpg2819 (see below), we termed the protein Lpg2819 "LppA" (*L*egionella *p*neumophila *p*hytase *A*).

LppA is not predicted to be secreted and has not been identified as an Icm/Dot T4SS substrate using bioinformatics or experimental approaches (49-52). To determine whether LppA is translocated by the Icm/Dot T4SS, we constructed an N-terminal fusion with the calmodulin-dependent adenylate cyclase CyaA that allows assessing the production of cAMP upon translocation of the fusion protein to host cell cytoplasm. To this end, RAW 246.7 macrophages were infected with either wild-type *L. pneumophila* or the translocation-defective Δ*icmT* mutant strain producing the CyaA-LppA fusion protein (Fig. 1B). Calmodulin-dependent production of cAMP was only observed upon infection with wild-type *L. pneumophila*, and therefore, LppA represents a hitherto unrecognized substrate of the Icm/Dot T4SS. Similarly, the positive control CyaA-RalF was translocated into the host cells in an Icm/Dot-dependent manner. These findings imply that LppA has access to the host cell cytoplasm and performs an intracellular function.

To test potential phytase activity of LppA, we performed a phosphate release assay and compared its activity to *S. ruminantium* PhyA. Under the conditions tested, purified GST-LppA hydrolyzed phytate at an initial rate of 5 pmol/s per µg protein, confirming its activity as an efficient phytase (Fig. 1C). The rate of GST-LppA was approximately twice as fast as GST-PhyA tested under these conditions. In order to determine the amino acids essential for enzymatic activity, we constructed point mutations in the putative catalytic motif. Mutations of the catalytic residues Cys231 or Arg237 to Ala resulted in loss of phytase activity (Fig. 1D). Moreover, replacing Gly236 with a more bulky and charged amino acid, Asp, also abolished phytate hydrolysis, whereas changing Lys235 to Ala did not alter the activity. Taken together, *L. pneumophila* produces a translocated cysteine phosphatase that *in vitro* shows a two-fold higher phytase activity than PhyA and harbors the conserved amino acids Cys_{215} and Arg_{221} implicated in catalysis.

LppA hydrolyses phosphoinositides in vitro and produces PtdIns(4)P - Given that inositol phosphates make up the identity-defining head group of PI lipids, we tested whether these derivatives of phytate could be metabolized by LppA *in vitro*. The P loop consensus sequence of the *L. pneumophila* phytase is similar to mammalian and bacterial PI phosphatases (Fig. 2A). In fact, the catalytically active site of LppA (HCRGGKGRT) is almost identical to the human PI 3-phosphatase PTEN (HCR/KAGKGRT) and very similar to the mycobacterial PI phosphatase MptpB (HCFAGKDRT). Therefore, we also tested the putative PI phosphatase activity of the enzyme towards di-octyl-PI lipids. LppA dephosphorylated the di-phosphorylated PIs PtdIns(3,4)P_2 and PtdIns(4,5)P_2 very efficiently, followed by

PtdIns(3,4,5)P_3 as a substrate and, with approximately 20 times lower activity, PtdIns(3,5)P_2 (Fig. 2B). A 100-fold higher amount of enzyme was required to observe poor activity towards mono-phosphorylated PIs (Fig. 2C).

To analyze the PI product(s) generated by LppA *in vitro*, we treated nitrocellulose membranes spotted with all 7 PIs and other lipids with the enzyme and subsequently performed a protein-lipid overlay using the PtdIns(4)*P*-specific probe GST-SidC$_{P4C}$ (Fig. 2D). GST-SidC$_{P4C}$ bound on untreated control membranes exclusively to the PtdIns(4)*P* spot as previously described (18). In contrast, on membranes pre-treated with LppA, GST-SidC$_{P4C}$ also bound to the spots initially occupied by PtdIns(3,4)P_2, PtdIns(4,5)P_2 or PtdIns(3,4,5)P_3, indicating that PtdIns(4)*P* is the major PI product of the phosphatase. In parallel, the LppA-treated membrane was probed with GST-LpnE to detect PtdIns(3)*P*. Yet, the fusion protein bound only to the initial PtdIns(3)*P* spot, indicating that no PtdIns(3)*P* was produced by the phosphatase LppA (Fig. 2E). Thus, *in vitro* LppA also rapidly metabolizes poly-phosphorylated PI lipids containing a 4-phosphate residue to yield PtdIns(4)*P*.

High-resolution structure of L. pneumophila LppA - Towards understanding LppA function at the molecular level, we determined the crystal structure of the phytase apo-form by molecular replacement at 1.4 Å resolution. The data collection and refinement statistics are listed in Table 3, and a structure-based alignment of LppA with PhyA is shown in Fig. 3A. The current model of LppA consists of amino-acid residues 26-314 (chain B in the unit cell tetramer) and reveals an overall structure of a mainly α-helical globular protein stabilized by four antiparallel β-sheets (Fig. 3B). The catalytic site forms a PTP-like fold characteristic of dual-specificity Ser/Thr and Tyr protein phosphatases.

One remarkable feature of the LppA crystal structure is the binding of two phosphate moieties in a positively charged pocket formed by the basic amino acids His203, Arg232, Lys235, Arg237 and Arg277. This pocket likely accommodates the binding sites for two out of the six phosphate residues of phytate. One phosphate localizes to the active site P-loop and is coordinated by the amino acids Cys231, Arg232, Lys235 and Arg237 (Fig. 3C). The position of Cys231 suggests a catalytic mechanism, where the thiolate anion of Cys231 is the nucleophile that attacks a phytate phosphate to form a cysteinyl-phosphate trigonal-bipyramidal pentavalent intermediate. The negative charge on the Sγ atom of Cys231 might be stabilized by the hydroxyl group of the conserved adjacent Thr238 (Fig. 2A). Also located in the catalytic pocket, Asp202 likely acts as a general acid and donates a proton to form *myo*-inositol pentakisphosphate. In the second step of the phosphatase reaction, Asp202 might act as a general base accepting a proton from a nearby water molecule (at a distance of 3.4 Å), which upon nucleophilic attack liberates phosphate and regenerates the active cysteinyl-phosphatase.

The second phosphate, which cannot be directly hydrolyzed, is coordinated by Gly236, Arg277 as well as Tyr286, and is further stabilized by His203 and the neighboring phosphate (Fig. 3D). The arrangement of the two adjacent phosphate moieties bound to LppA is in agreement with a model proposed for the phytase PhyA from *S. ruminantium*, suggesting that after hydrolytic removal of the first phosphate, *myo*-inositol pentakisphosphate rotates and a second phosphate is placed in vicinity to the catalytically active cysteine to be subsequently hydrolyzed in a step-wise manner (39).

Comparison of L. pneumophila LppA and S. ruminantium PhyA - The phytase LppA is structurally similar to the *S. ruminantium* phytase PhyA in its apo form (PDB code 1U24). C_α superimposition of PhyA onto LppA results in an rmsd of 1.6 Å over 254 residues and 28% sequence identity (Fig. 4A). Significant differences in structure are seen at the N and C termini that extend by 11 and 9 residues in PhyA, respectively. Furthermore, LppA is lacking a loop present in PhyA (amino acids 88-99). These results are in good agreement with the overall similarity of LppA and PhyA, which share 30% sequence identity.

The P-loop sites of LppA (HCRGGKGRT) and PhyA (HCEAGVGRT) are 66% identical, and the phosphate groups bound by LppA superimposes with S4 and S5 of the inhibitor *myo*-inositol hexasulfate (IHS) that was co-crystallized with PhyA from *S. ruminantium* (PDB code 1U26) (Fig. 4B). Noteworthy, Arg232 and Arg277 coordinating in LppA the phosphate residues in the catalytic or the non-catalytic site, respectively, are replaced by an acidic amino acid in PhyA (Glu242 and Asp289). Moreover, LppA Lys235 is not

conserved in PhyA, and accordingly, its replacement by Ala did not affect the catalytic activity of LppA (Fig. 1D). In contrast, mutation of PhyA His213 or Tyr298, which form the substrate-binding pocket and are conserved in LppA (His187 and Tyr270), caused a significant decrease in phytase activity by 52% and 92%, respectively (39). In summary, these findings suggest a similar mechanism of phytate binding and catalysis of LppA and PhyA.

Phytate reversibly inhibits L. pneumophila growth and is counteracted by LppA or micro-nutrient supplementation - To investigate the effect of phytate on the growth of *L. pneumophila* in AYE broth, the compound was added to a bacterial culture in early exponential growth phase (Fig. 5A). Under these conditions, 10 mM phytate caused growth stasis of *L. pneumophila*. The bacteria were subsequently pelleted, suspended in fresh AYE medium and let grow again. After phytate was removed, *L. pneumophila* resumed growth at the initial rate. Therefore, phytate is not toxic to *L. pneumophila*, but reversibly inhibits growth of *L. pneumophila* and thus exerts a bacteriostatic rather than a bactericidal effect.

Next, we thought to assess the effect of LppA on growth inhibition by phytate. To this end, an *L. pneumophila* mutant strains lacking *lppA* (Δ*lppA*) was generated by double homologous recombination. Western blots using a polyclonal anti-LppA antibody revealed that the Δ*lppA* mutant strain did not produce LppA anymore, yet phytase production was restored upon expression of plasmid-encoded *lppA* (pWS31) (Fig. 5B, data not shown). Moreover, upon overproduction of LppA by wild-type *L. pneumophila* some phytase was detected in the supernatants of bacterial cultures. Growth of *L. pneumophila* wild-type, Δ*lppA*, or wild-type overproducing LppA in AYE medium supplemented with 0-5 mM phytate was monitored by measuring the optical density of the culture. In absence of phytate, the *L. pneumophila* strains grew indistinguishably. The addition of phytate inhibited bacterial growth in a dose-dependent manner, and 5 mM of the compound completely abolished bacterial replication (Fig. 5C). *L. pneumophila* lacking *lppA* was slightly more susceptible towards phytate upon growth at 24°C, but not at 37°C, regardless of whether complex AYE or chemically defined minimal medium was used (data not shown). On the other hand, the wild-type strain overproducing LppA grew significantly better at phytate concentrations ranging from 1-4 mM. Thus, LppA phytase (released from the bacteria) counteracts the bacteriostatic effect of phytate (Fig. 5B, 5C).

Phytate is a strong chelator and complexes iron, calcium, zinc, and magnesium among other micro-nutrients (37). In order to test whether the bacteriostatic effect of phytate on *L. pneumophila* is due to its chelating properties, we added the compound in presence of equimolar concentrations of micro-nutrients (iron, zinc, magnesium or calcium) to bacterial cultures growing in AYE medium and assessed growth. Whereas 10 mM phytate (or the positive control EDTA) completely blocked the growth of *L. pneumophila*, the concomitant addition of 10 mM of micro-nutrients reversed the inhibition (Fig. 5D). In summary, supplementation of phytate with equimolar concentrations of metal ions reversed the bacteriostatic effects of phytate, and therefore, growth inhibition is due to micro-nutrient deprivation by the chelator.

LppA promotes intracellular replication of L. pneumophila in phytate-loaded amoebae - To determine whether phytate plays a role for intracellular replication of *L. pneumophila*, we pre-loaded *A. castellanii* or *D. discoideum* with the chelator. To this end, the amoebae were initially treated with 2.5 mM phytate, and the concentration was increased every two days up to 10 mM for *A. castellanii* or 5 mM for *D. discoideum*. Shortly before an experiment, the amoebae were washed and suspended in LoFlo medium. The phytate-loaded amoebae were then infected with GFP-producing *L. pneumophila* wild-type, Δ*icmT*, Δ*lppA* or complemented Δ*lppA* strains. Bright field and GFP-fluorescence microscopy images were taken for infected *A. castellanii*.

Images immediately following infection show an even distribution of amoebae and *L. pneumophila* (Fig. 6A). After 48 h, amoebae infected with wild-type *L. pneumophila* or the complemented Δ*lppA* mutant strain predominantly had rounded up, which is a characteristic of advanced *L. pneumophila* infection. The bright field channel shows that the majority of the cells are filled with bacteria, many of which are producing GFP. The synthesis of GFP was rather low and heterogeneous for the complementation strain producing a short-lived GFP. In contrast, amoebae infected with *L. pneumophila* lacking *lppA* remained largely attached, the morphology of

most amoebae was similar to cells infected with Δ*icmT*, and only a few amoebae were observably filled with bacteria. By 72 h post infection, *A. castellanii* infected with wild-type *L. pneumophila* were full of actively moving bacteria ready for exit (Movie S1), and many amoebae infected with the complemented Δ*lppA* mutant strain had burst, releasing the intracellular bacteria (Movie S2). Replication of the Δ*lppA* mutant strain increased over the 48 h time point, but was still considerably lower than replication by wild-type or complementation strains (Movie S3), and many cells resembled the Δ*icmT*-infected amoebae (Movie S4).

Intracellular growth of the *L. pneumophila* strains in phytate-loaded *A. castellanii* or *D. discoideum* was also quantified by determining colony forming units (CFU) (Fig. 6B, 6C). Colony counts at the onset of infection were even across all strains, and Δ*icmT* mutant bacteria used as a negative control disappeared over time. Using CFU as readout for intracellular replication, significantly fewer bacteria lacking *lppA* were counted after 48 or 72 h infection, and the growth defect was fully complemented by providing the gene on a plasmid.

We also tested the possible role of *lppA* for intracellular growth of *L. pneumophila* in *A. castellanii* or *D. discoideum* cultured in absence of phytate. To this end, the amoebae were grown in standard media, infected with *L. pneumophila* wild-type, Δ*icmT*, Δ*lppA* or complemented Δ*lppA* strains, and intracellular growth was determined by CFU after 48 h infection. However, under these conditions, the deletion or overexpression of *lppA* did not affect intracellular bacterial growth (Fig. 6D, data not shown). Moreover, upon co-infection of *A. castellanii* with *L. pneumophila* wild-type and Δ*lppA* at a 1:1 ratio, the mutant strain was not outcompeted for up to 18 days (data not shown). Finally, *lppA* did not affect the growth of *L. pneumophila* in RAW264.7 macrophages, for which phytate was toxic (data not shown). In summary, these findings indicated that the *L. pneumophila* translocated phytase LppA provides an intracellular growth advantage in phytate-loaded amoebae such as *A. castellanii* or *D. discoideum*.

LppA does not play a major role for the modulation of the LCV PI pattern - LppA is translocated into host cells and *in vitro* efficiently hydrolyzes PI lipids to yield PtdIns(4)*P* (Fig. 2). Thus, we hypothesized that LppA might also modulate the LCV PI pattern in *L. pneumophila*-infected cells. To compare the dynamics of PtdIns(4)*P* accumulation on LCVs harboring wild-type or Δ*lppA* mutant bacteria, we performed live cell imaging using specific PI probes (21). Upon infection of *D. discoideum* amoebae producing GFP-SidC$_{P4C}$ with *L. pneumophila*, LCVs harboring wild-type or Δ*lppA* bacteria accumulated PtdIns(4)*P* to the same extent within 1 or 2 h post infection (Fig. 7A, 7B). The LCVs were similar in size and GFP-SidC$_{P4C}$ signal intensity, and PtdIns(4)*P* persisted on LCVs containing replicating bacteria. Similar results were obtained upon staining the endogenously produced PtdIns(4)*P*-binding effector SidC on LCVs harboring wild-type or Δ*lppA L. pneumophila* (data not shown). Finally, LCVs harboring *L. pneumophila* wild-type or Δ*lppA* mutant bacteria were decorated to the same extent with the ER marker calnexin (data not shown). Taken together, the translocated *L. pneumophila* phytase LppA does not appear to modulate the LCV PI pattern in infected cells.

DISCUSSION

In this study we identified the chelator phytate as an intracellular bacteriostatic compound, and we provide evidence that the T4SS-translocated *L. pneumophila* phytase LppA counteracts bacterial growth restriction by phytate by hydrolyzing and thus inactivating the chelator. *L. pneumophila* requires iron for growth (53), and accordingly, the standard growth medium AYE contains 0.6 mM iron. The bacteria possess a number of iron uptake systems, including the siderophore legiobactin and the ferrous iron transmembrane transporter FeoB (54). The requirement for iron and possibly other micro-nutrients provides a rationale for the susceptibility of *L. pneumophila* towards the chelator phytate (Fig. 5). The sensitivity of *L. pneumophila* towards phytate also suggests that under the conditions tested, the bacteria do not use phytate as a source of phosphorus or as a siderophore for micro-nutrients, which has been described for *X. oryzae* (34) or *P. aeruginosa* (35,36), respectively.

Upon extracellular growth in AYE broth, an *L. pneumophila* strain lacking *lppA* was only slightly more susceptible towards phytate. The mild phenotype was observed only at a low growth temperature of 24°C, but not at 37°C, regardless of

whether complex AYE or chemically defined minimal medium was used (data not shown). In contrast, the wild-type strain overproducing LppA grew significantly better in presence of 1-4 mM phytate (Fig. 5C). The overproduction of LppA resulted in a portion of the phytase being released by the bacteria (Fig. 5B). Therefore, these findings are in agreement with the notion that LppA in the growth medium counteracts the bacteriostatic effect of phytate. The poly-anionic compound phytate is expected to be largely membrane-impermeable and might not be taken up actively by *L. pneumophila*. Hence, under extracellular conditions where LppA is not translocated into a host cell, the absence of the phytase does not result in a pronounced growth defect.

Amoebae, and in particular the social soil amoeba *D. discoideum*, produce phytate in the millimolar range (31-33). Phytate concentrations above 1-2 mM inhibit the extracellular growth of *L. pneumophila* (Fig. 5C), very likely due to the chelation of micro-nutrients (Fig. 5D). It is challenging to quantify the intracellular concentrations of micro-nutrients and the intracellular micro-nutrient requirements of *L. pneumophila* in host cells. Yet the intracellular production of phytate in millimolar quantities seems sufficient to reduce or even deplete from pathogen-accessible intracellular compartments the micro-nutrients essential for *L. pneumophila*. We showed that *D. discoideum* as well as *A. castellanii* pre-loaded with phytate (but not amoebae grown in standard media) restrict intracellular growth of *L. pneumophila* in an *lppA*-dependent manner (Fig. 6). Perhaps, the micro-nutrients available under the laboratory conditions used over-compensated the endogenous phytate produced by the amoeba.

Protozoa take up solutes via macropinocytic processes, and the macropinosomes formed likely communicate with LCVs. In support of this notion, *L. pneumophila* itself is taken up by phagocytes by macropinocytic rather than phagocytic processes (21,55). Thus, the exogenously added phytate might reach the pathogen compartment through vesicle fusion; yet transmembrane transport processes might also play a role. Notably, the obligate intra-amoebal bacterium *Candidatus Protochlamydia amoebophila*, produces a putative cysteine phytase (32% identity with LppA) (29). This finding suggests that the phytate-containing compartment communicates with the bacterial symbiont, and that degradation of intracellular phytate might also be beneficial for survival and replication of this bacterium.

Whereas LppA hydrolyzes phytate as well as poly-phosphorylated PI lipids *in vitro*, only the phytase activity appears to be relevant in infected cells (Fig. 6, 7). Other *L. pneumophila* Icm/Dot substrates, such as the PI phosphatases SidF and SidP, as well as host PI-metabolizing enzymes seem to modulate and define the LCV PI pattern. This is consistent with the notion that LppA apparently plays only a minor if any role in LCV formation. Cysteine phytases are characterized by the catalytic motif HCX_2GX_2R, of which the Cys and Arg residues are catalytically essential and His and Gly are important for conformation of the P-loop (39). While the catalytic motif of LppA (HCRGGKGRT) is 66% identical to PhyA (HCEAGVGRT), it shares 89% identity with the mammalian PI 3-phosphatase PTEN (HCR/KAGKGRT) (Fig. 2A). Since both PTEN and LppA (Fig. 2B) effectively metabolize PtdIns(3,4,5)P_3 and the main PI product of LppA *in vitro* is PtdIns(4)*P* (Fig. 2D, 2E), it is tantalizing that LppA apparently does not function as a PI phosphatase in infected cells.

The results obtained in this study emphasize the critical role of micro-nutrients for intracellular pathogens. As an anti-bacterial strategy against vacuolar pathogens, micro-nutrient depletion by the chelator phytate might function in parallel with transporters that remove metal ions from the pathogen vacuole. Accordingly, the transmembrane proteins Nramp-1 and Nramp-2 have been shown to pump iron from vacuoles (LCV) to the cytoplasm of *D. discoideum* (56,57). While the eukaryotic cell limits the availability of micro-nutrients by producing chelators and ion pumps, the intracellular pathogen *L. pneumophila* developed means to counteract the bacteriostatic strategy. Thus, our study reveals the potential to exploit intracellular micro-nutrient deprivation as an anti-bacterial strategy. Specifically, phytases or other microbial chelator antagonists might represent targets to control intracellular growth and virulence of bacterial pathogens.

REFERENCES

1. Newton, H. J., Ang, D. K., van Driel, I. R., and Hartland, E. L. (2010) Molecular pathogenesis of infections caused by *Legionella pneumophila*. *Clin Microbiol Rev* **23**, 274-298
2. Hilbi, H., Hoffmann, C., and Harrison, C. F. (2011) *Legionella* spp. outdoors: colonization, communication and persistence. *Environ Microbiol Rep* **3**, 286–296
3. Whiley, H., and Bentham, R. (2011) *Legionella longbeachae* and legionellosis. *Emerg Infect Dis* **17**, 579-583
4. Hoffmann, C., Harrison, C. F., and Hilbi, H. (2013) The natural alternative: protozoa as cellular models for *Legionella* infection. *Cell Microbiol* **16**, 15-26
5. Isberg, R. R., O'Connor, T. J., and Heidtman, M. (2009) The *Legionella pneumophila* replication vacuole: making a cosy niche inside host cells. *Nat Rev Microbiol* **7**, 13-24
6. Hubber, A., and Roy, C. R. (2010) Modulation of host cell function by *Legionella pneumophila* type IV effectors. *Annu Rev Cell Dev Biol* **26**, 261-283
7. Hilbi, H., and Haas, A. (2012) Secretive bacterial pathogens and the secretory pathway. *Traffic* **13**, 1187-1197
8. Itzen, A., and Goody, R. S. (2011) Covalent coercion by *Legionella pneumophila*. *Cell Host Microbe* **10**, 89-91
9. Sherwood, R. K., and Roy, C. R. (2013) A Rab-centric perspective of bacterial pathogen-occupied vacuoles. *Cell Host Microbe* **14**, 256-268
10. Rothmeier, E., Pfaffinger, G., Hoffmann, C., Harrison, C. F., Grabmayr, H., Repnik, U., Hannemann, M., Wölke, S., Bausch, A., Griffiths, G., Müller-Taubenberger, A., Itzen, A., and Hilbi, H. (2013) Activation of Ran GTPase by a *Legionella* effector promotes microtubule polymerization, pathogen vacuole motility and infection. *PLoS Pathog* **9**, e1003598
11. Hoffmann, C., Finsel, I., Otto, A., Pfaffinger, G., Rothmeier, E., Hecker, M., Becher, D., and Hilbi, H. (2013) Functional analysis of novel Rab GTPases identified in the proteome of purified *Legionella*-containing vacuoles from macrophages. *Cell Microbiol* **16**, 1034-52
12. Simon, S., Wagner, M. A., Rothmeier, E., Müller-Taubenberger, A., and Hilbi, H. (2014) Icm/Dot-dependent inhibition of phagocyte migration by *Legionella* is antagonized by a translocated Ran GTPase activator. *Cell Microbiol* **16**, 977-92
13. Hilbi, H., Rothmeier, E., Hoffmann, C., and Harrison, C. F. (2014) Beyond Rab GTPases: *Legionella* activates the small GTPase Ran to promote microtubule polymerization, pathogen vacuole motility, and infection. *Small GTPases* **5**, Epub ahead of print
14. Ham, H., Sreelatha, A., and Orth, K. (2011) Manipulation of host membranes by bacterial effectors. *Nat Rev Microbiol* **9**, 635-646
15. Hilbi, H., Weber, S., and Finsel, I. (2011) Anchors for effectors: subversion of phosphoinositide lipids by *Legionella*. *Front Microbiol* **2**, 91
16. Haneburger, I., and Hilbi, H. (2013) Phosphoinositide lipids and the *Legionella* pathogen vacuole. *Curr Top Microbiol Immunol* **376**, 155-173
17. Weber, S. S., Ragaz, C., Reus, K., Nyfeler, Y., and Hilbi, H. (2006) *Legionella pneumophila* exploits PI(4)*P* to anchor secreted effector proteins to the replicative vacuole. *PLoS Pathog* **2**, e46
18. Ragaz, C., Pietsch, H., Urwyler, S., Tiaden, A., Weber, S. S., and Hilbi, H. (2008) The *Legionella pneumophila* phosphatidylinositol-4-phosphate-binding type IV substrate SidC recruits endoplasmic reticulum vesicles to a replication-permissive vacuole. *Cell Microbiol* **10**, 2416-2433
19. Brombacher, E., Urwyler, S., Ragaz, C., Weber, S. S., Kami, K., Overduin, M., and Hilbi, H. (2009) Rab1 guanine nucleotide exchange factor SidM is a major phosphatidylinositol 4-phosphate-binding effector protein of *Legionella pneumophila*. *J Biol Chem* **284**, 4846-4856
20. Schoebel, S., Blankenfeldt, W., Goody, R. S., and Itzen, A. (2010) High-affinity binding of phosphatidylinositol 4-phosphate by *Legionella pneumophila* DrrA. *EMBO Rep* **11**, 598-604
21. Weber, S., Wagner, M., and Hilbi, H. (2014) Live cell imaging of phosphoinositide dynamics and membrane architecture during *Legionella* infection. *mBio* **5**, e00839-13

22. Dolinsky, S., Haneburger, I., Cichy, A., Hannemann, M., Itzen, A., and Hilbi, H. (2014) The *Legionella longbeachae* Icm/Dot substrate SidC selectively binds PtdIns(4)*P* with nanomolar affinity and promotes pathogen vacuole-ER interactions. *Infect Immun*, Epub ahead of print
23. Weber, S. S., Ragaz, C., and Hilbi, H. (2009) The inositol polyphosphate 5-phosphatase OCRL1 restricts intracellular growth of *Legionella*, localizes to the replicative vacuole and binds to the bacterial effector LpnE. *Cell Microbiol* **11**, 442-460
24. Jank, T., Bohmer, K. E., Tzivelekidis, T., Schwan, C., Belyi, Y., and Aktories, K. (2012) Domain organization of *Legionella* effector SetA. *Cell Microbiol* **14**, 852-868
25. Finsel, I., Ragaz, C., Hoffmann, C., Harrison, C. F., Weber, S., van Rahden, V. A., Johannes, L., and Hilbi, H. (2013) The *Legionella* effector RidL inhibits retrograde trafficking to promote intracellular replication. *Cell Host Microbe* **14**, 38-50
26. Hsu, F., Zhu, W., Brennan, L., Tao, L., Luo, Z. Q., and Mao, Y. (2012) Structural basis for substrate recognition by a unique *Legionella* phosphoinositide phosphatase. *Proc Natl Acad Sci U S A* **109**, 13567-13572
27. Toulabi, L., Wu, X., Cheng, Y., and Mao, Y. (2013) Identification and structural characterization of a *Legionella* phosphoinositide phosphatase. *J Biol Chem* **288**, 24518-24527
28. Turner, B. L., Paphazy, M. J., Haygarth, P. M., and McKelvie, I. D. (2002) Inositol phosphates in the environment. *Philos Trans R Soc Lond B Biol Sci* **357**, 449-469
29. Lim, B. L., Yeung, P., Cheng, C., and Hill, J. E. (2007) Distribution and diversity of phytate-mineralizing bacteria. *ISME J* **1**, 321-330
30. Rao, D. E., Rao, K. V., Reddy, T. P., and Reddy, V. D. (2009) Molecular characterization, physicochemical properties, known and potential applications of phytases: An overview. *Crit Rev Biotechnol* **29**, 182-198
31. Martin, J. B., Foray, M. F., Klein, G., and Satre, M. (1987) Identification of inositol hexaphosphate in ^{31}P-NMR spectra of *Dictyostelium discoideum* amoebae. Relevance to intracellular pH determination. *Biochim Biophys Acta* **931**, 16-25
32. Stephens, L. R., and Irvine, R. F. (1990) Stepwise phosphorylation of *myo*-inositol leading to *myo*-inositol hexakisphosphate in *Dictyostelium*. *Nature* **346**, 580-583
33. Pisani, F., Livermore, T., Rose, G., Chubb, J. R., Gaspari, M., and Saiardi, A. (2014) Analysis of *Dictyostelium discoideum* inositol pyrophosphate metabolism by gel electrophoresis. *PLoS One* **9**, e85533
34. Chatterjee, S., Sankaranarayanan, R., and Sonti, R. V. (2003) PhyA, a secreted protein of *Xanthomonas oryzae* pv. *oryzae*, is required for optimum virulence and growth on phytic acid as a sole phosphate source. *Mol Plant Microbe Interact* **16**, 973-982
35. Smith, A. W., Poyner, D. R., Hughes, H. K., and Lambert, P. A. (1994) Siderophore activity of *myo*-inositol hexakisphosphate in *Pseudomonas aeruginosa*. *J Bacteriol* **176**, 3455-3459
36. Hirst, P. H., Riley, A. M., Mills, S. J., Spiers, I. D., Poyner, D. R., Freeman, S., Potter, B. V., and Smith, A. W. (1999) Inositol polyphosphate-mediated iron transport in *Pseudomonas aeruginosa*. *J Appl Microbiol* **86**, 537-543
37. Urbano, G., Lopez-Jurado, M., Aranda, P., Vidal-Valverde, C., Tenorio, E., and Porres, J. (2000) The role of phytic acid in legumes: antinutrient or beneficial function? *J Physiol Biochem* **56**, 283-294
38. Mullaney, E. J., and Ullah, A. H. (2003) The term phytase comprises several different classes of enzymes. *Biochem Biophys Res Commun* **312**, 179-184
39. Chu, H. M., Guo, R. T., Lin, T. W., Chou, C. C., Shr, H. L., Lai, H. L., Tang, T. Y., Cheng, K. J., Selinger, B. L., and Wang, A. H. (2004) Structures of *Selenomonas ruminantium* phytase in complex with persulfated phytate: DSP phytase fold and mechanism for sequential substrate hydrolysis. *Structure* **12**, 2015-2024
40. Norris, F. A., Wilson, M. P., Wallis, T. S., Galyov, E. E., and Majerus, P. W. (1998) SopB, a protein required for virulence of *Salmonella dublin*, is an inositol phosphate phosphatase. *Proc Natl Acad Sci U S A* **95**, 14057-14059
41. Wishart, M. J., and Dixon, J. E. (2002) PTEN and myotubularin phosphatases: from 3-phosphoinositide dephosphorylation to disease. *Trends Cell Biol* **12**, 579-585

42. Grundner, C., Ng, H. L., and Alber, T. (2005) *Mycobacterium tuberculosis* protein tyrosine phosphatase PtpB structure reveals a diverged fold and a buried active site. *Structure* **13**, 1625-1634
43. Beresford, N., Patel, S., Armstrong, J., Szoor, B., Fordham-Skelton, A. P., and Tabernero, L. (2007) MptpB, a virulence factor from *Mycobacterium tuberculosis*, exhibits triple-specificity phosphatase activity. *Biochem J* **406**, 13-18
44. Tiaden, A., Spirig, T., Weber, S. S., Brüggemann, H., Bosshard, R., Buchrieser, C., and Hilbi, H. (2007) The *Legionella pneumophila* response regulator LqsR promotes host cell interactions as an element of the virulence regulatory network controlled by RpoS and LetA. *Cell Microbiol* **9**, 2903-2920
45. Studier, F. W. (2005) Protein production by auto-induction in high density shaking cultures. *Prot Expr Purif* **41**, 207-234
46. Chen, J., de Felipe, K. S., Clarke, M., Lu, H., Anderson, O. R., Segal, G., and Shuman, H. A. (2004) *Legionella* effectors that promote nonlytic release from protozoa. *Science* **303**, 1358-1361
47. Kessler, A., Schell, U., Sahr, T., Tiaden, A., Harrison, C., Buchrieser, C., and Hilbi, H. (2013) The *Legionella pneumophila* orphan sensor kinase LqsT regulates competence and pathogen-host interactions as a component of the LAI-1 circuit. *Environ Microbiol* **15**, 646-662
48. Puhl, A. A., Gruninger, R. J., Greiner, R., Janzen, T. W., Mosimann, S. C., and Selinger, L. B. (2007) Kinetic and structural analysis of a bacterial protein tyrosine phosphatase-like *myo*-inositol polyphosphatase. *Prot Sci* **16**, 1368-1378
49. Heidtman, M., Chen, E. J., Moy, M. Y., and Isberg, R. R. (2009) Large-scale identification of *Legionella pneumophila* Dot/Icm substrates that modulate host cell vesicle trafficking pathways. *Cell Microbiol* **11**, 230-248
50. Burstein, D., Zusman, T., Degtyar, E., Viner, R., Segal, G., and Pupko, T. (2009) Genome-scale identification of *Legionella pneumophila* effectors using a machine learning approach. *PLoS Pathog* **5**, e1000508
51. Zhu, W., Banga, S., Tan, Y., Zheng, C., Stephenson, R., Gately, J., and Luo, Z. Q. (2011) Comprehensive identification of protein substrates of the Dot/Icm type IV transporter of *Legionella pneumophila*. *PLoS One* **6**, e17638
52. Lifshitz, Z., Burstein, D., Peeri, M., Zusman, T., Schwartz, K., Shuman, H. A., Pupko, T., and Segal, G. (2013) Computational modeling and experimental validation of the *Legionella* and *Coxiella* virulence-related type-IVB secretion signal. *Proc Natl Acad Sci U S A* **110**, E707-715
53. Reeves, M. W., Pine, L., Hutner, S. H., George, J. R., and Harrell, W. K. (1981) Metal requirements of *Legionella pneumophila*. *J Clin Microbiol* **13**, 688-695
54. Cianciotto, N. P. (2007) Iron acquisition by *Legionella pneumophila*. *Biometals* **20**, 323-331
55. Peracino, B., Balest, A., and Bozzaro, S. (2010) Phosphoinositides differentially regulate bacterial uptake and Nramp1-induced resistance to *Legionella* infection in *Dictyostelium*. *J Cell Sci* **123**, 4039-4051
56. Bozzaro, S., Buracco, S., and Peracino, B. (2013) Iron metabolism and resistance to infection by invasive bacteria in the social amoeba *Dictyostelium discoideum*. *Front Cell Inf Microbiol* **3**, 50
57. Peracino, B., Buracco, S., and Bozzaro, S. (2013) The Nramp (Slc11) proteins regulate development, resistance to pathogenic bacteria and iron homeostasis in *Dictyostelium discoideum*. *J Cell Sci* **126**, 301-311
58. Segal, G., and Shuman, H. A. (1998) Intracellular multiplication and human macrophage killing by *Legionella pneumophila* are inhibited by conjugal components of IncQ plasmid RSF1010. *Mol Microbiol* **30**, 197-208
59. Sadosky, A. B., Wiater, L. A., and Shuman, H. A. (1993) Identification of *Legionella pneumophila* genes required for growth within and killing of human macrophages. *Infect Immun* **61**, 5361-5373
60. Wiater, L. A., Sadosky, A. B., and Shuman, H. A. (1994) Mutagenesis of *Legionella pneumophila* using Tn*903*dll*lacZ*: identification of a growth-phase-regulated pigmentation gene. *Mol Microbiol* **11**, 641-653

61. Mampel, J., Spirig, T., Weber, S. S., Haagensen, J. A. J., Molin, S., and Hilbi, H. (2006) Planktonic replication is essential for biofilm formation by *Legionella pneumophila* in a complex medium under static and dynamic flow conditions. *Appl Environ Microbiol* **72**, 2885-2895

ACKNOWLEDGEMENTS

We would like to thank Aline Kessler and Sabrina Heiny for constructing pAK7 and pSH108, respectively. The work in the group of H. H. was funded by the Max von Pettenkofer Institute, Ludwig-Maximilians University Munich, the German Research Foundation (DFG; HI 1511/1-1, SPP 1316, SPP 1580) and the German Ministry of Education and Research (BMBF) in the context of the Infect-ERA initiative (project EUGENPATH). C. U. S., X. L., G. C. and R. A. K. were funded by the Paul Scherrer Institute and grants from the Swiss National Science Foundation (SNF). The funders had no role in study design, data collection and analysis, decision to publish, or preparation of the manuscript.

FIGURE LEGENDS

FIGURE 1. The type-IV translocated cysteine phosphatase LppA hydrolyses phytate *in vitro*. *(A)* Alignment of (predicted) cysteine phytases of *Legionella pneumophila* (LppA), *Legionella longbeachae*, *Stigmatella aurantica*, *Clostridium acetobutylicum* and *Selenomonas ruminantium* (PhyA) in order of decreasing homology to LppA. The red box highlights the established or predicted P-loop catalytic active sites for LppA and PhyA, as well as for the other putative phytases. (*B*) LppA is a substrate of the Icm/Dot T4SS. RAW 264.7 macrophages were infected with wild-type or Δ*icmT L. pneumophila* harboring pSH108 (CyaA-LppA) or pSH100 (CyaA-RalF). Levels of cAMP (mean ± SD, four duplicate experiments) were measured 30 min post infection (MOI 50). (*C*, *D*) Hydrolysis of phytate by GST-$LppA_{\Delta 1\text{-}16}$, GST-PhyA or GST-$LppA_{\Delta 1\text{-}16}$ point mutations of putative catalytically essential residues was measured by phosphate release as a malachite green vanadate dye complex. Reactions proceeded at 25°C with 2 nmol phytate and 0.5 µg protein for up to (*C*) 10 min or (*D*) 15 min. Absorbance at 620 nm was measured 20 min after termination of each reaction. The data shown are means and standard deviation (SD) of triplicates (*B-D*) and are representative of three independent experiments (** $P < 0.005$).

FIGURE 2. LppA hydrolyses phosphoinositides and produces PtdIns(4)*P in vitro*. (*A*) Alignment of P-loops of bacterial and eukaryotic cysteine phytases and phosphoinositide phosphatases: *L. pneumophila* (LppA, SidF, SidP), *S. ruminantium* (PhyA), *M. tuberculosis* (MptpB), *H. sapiens* (PTEN). (*B*, *C*) Hydrolysis of PI lipids by $LppA_{\Delta 1\text{-}16}$ was measured by phosphate release as a malachite green vanadate dye complex with 1 nmol di-octyl PI lipids and (*B*) 0.05 µg or (*C*) 5 µg protein, respectively. (*D*, *E*) LppA hydrolyzes polyphosphorylated PIs and produces PtdIns(4)*P* but not PtdIns(3)*P*. Nitrocellulose membranes with PI and other lipids (100 pmol/spot) were (*D*) treated (right panel) or not (left panel) with purified $LppA_{\Delta 1\text{-}16}$ (0.5 µg/µl, 10 min), prior to binding of the PtdIns(4)*P* probe GST-$SidC_{P4C}$, or *(E)* treated with purified $LppA_{\Delta 1\text{-}16}$ (0.5 µg/µl, 10 min) and overlayed with the PtdIns(3)*P* probe GST-LpnE (left panel), followed by washing and overlaying with GST-$SidC_{P4C}$ (right panel). Binding was visualized using an anti-GST antibody. Left lanes (all membranes): lysophosphatidic (LPA), lysophosphocholine (LPC), phosphatidylinositol (PtdIns), phosphoinositide (PtdIns(x)*P*), phosphatidylethanolamine (PE), phosphatidylcholine (PC). Right lanes (all membranes): sphingosine-1-phosphate (S1*P*), phosphoinositide (PtdIns(x)*P*), phosphatidic acid (PA), phosphatidylserine (PS). The data shown are representative of three independent experiments.

FIGURE 3. Overall structure of *L. pneumophila* LppA bound to two phosphates. (*A*) Structure-based alignment of *L. pneumophila* LppA with *S. ruminantium* PhyA. (*B*) Overall structure of LppA showing 2 bound phosphates (phosphorus: orange, oxygen: red). (*C*) Close-up view of the catalytic P-loop site of LppA coordinating a phosphate with the amino acids Asp202, Cys231, Arg232, Lys235, Arg237 and

Thr238. (*D*) Close-up view of the second phosphate coordinated at a non-catalytic site by Gly236, Arg277 and Tyr286.

FIGURE 4. Comparison of overall structure and active sites of *L. pneumophila* LppA and *S. ruminantium* PhyA. (*A*) Overlay of the overall structures and (*B*) close-up view of the catalytic P-loop sites of *L. pneumophila* LppA (green) and *S. ruminantium* PhyA (red) bound to 2 phosphates (green) or the inhibitor myo-inositol hexasulfate (IHS; red), respectively.

FIGURE 5. Phytate reversibly inhibits *L. pneumophila* growth and is counteracted by LppA or micro-nutrient supplementation. (*A*) Phytate is bacteriostatic for *L. pneumophila*. Wild-type *L. pneumophila* was inoculated at an OD_{600} of 0.1 in AYE medium, and growth was measured by OD_{600} every 3 h from 12-30 h. At 12 h 10 mM phytate (InsP_6) was added for 6 h (dashed line), the bacteria were pelleted, resuspended in fresh AYE medium and let grow again. The control without phytate was treated the same way. (*B*) Detection of LppA by Western blot in *L. pneumophila* wild-type or Δ*lppA* harboring pCR33 (vector), wild-type harboring pRM1 (M45-LppA) and culture supernatants. The data shown are representative of two independent experiments. (*C*) Growth inhibition by phytate is counteracted by LppA. *L. pneumophila* wild-type or Δ*lppA* harboring pCR33 (vector), or wild-type harboring pRM1 (M45-LppA) were grown in AYE supplemented with 0-5 mM InsP_6 for 5 d at 24°C. (*D*) Micronutrient supplementation of *L. pneumophila* cultures grown with 10 mM InsP_6. *L. pneumophila* was grown for 21 h in AYE containing 10 mM InsP_6 or 10 mM of the micro-nutrients indicated (iron, zinc, magnesium or calcium). 10 mM EDTA alone was used as a control for chelation. Data (A-C) represent means ± SD of triplicates (*P < 0.05, **P < 0.005).

FIGURE 6. LppA promotes intracellular replication of *L. pneumophila* under phytate load. *(A) A. castellanii* amoebae cultured in presence of 10 mM phytate were infected (MOI 1, 37°C) with *L. pneumophila* wild-type, Δ*lppA* or Δ*icmT* harboring pNT28 (GFP), or Δ*lppA* harboring pWS31 (GFP, LppA). Bright field and GFP fluorescence images for infected *A. castellanii* taken at 0, 48 or 72 h post infection. Scale bar, 50 µm. (*B*) CFU counts for intracellular replication of *L. pneumophila* strains corresponding to images in *(A)*. (*C*) CFU counts for intracellular replication of above-listed *L. pneumophila* strains at 23°C in *D. discoideum* pre-loaded with 5 mM phytate. Data represent means ± SD of triplicates and are representative of three independent experiments (*p < 0.05, ** p < 0.005). (*D*) *A. castellanii* cultured in absence of phytate was infected (MOI 1, 37° C) with *L. pneumophila* wild-type, Δ*lppA* or Δ*icmT* harboring pNT28 (GFP), or Δ*lppA* harboring pWS31 (GFP, LppA), and intracellular growth was determined by CFU at 0 and 48 h post infection.

FIGURE 7. LppA does not influence the LCV PtdIns(4)*P* pattern in infected phagocytes. *(A)* Live cell imaging of *D. discoideum* producing GFP-$SidC_{P4C}$ infected with wild-type or Δ*lppA L. pneumophila* (pSW1, DsRed) at an MOI 10. Images were taken 2 h post infection at 23°C. Scale bars, 5 µm. *(B)* Quantification of PtdIns(4)*P*-positive LCVs. At least 100 LCVs were counted for each sample 2 h post infection Scale bar, 5 µm.

MOVIE S1. *A. castellanii* infected with *L. pneumophila* wild-type/pNT28 (72 h post infection, bright field).

MOVIE S2. *A. castellanii* infected with *L. pneumophila* Δ*lppA*/pWS31 (72 h post infection, bright field).

MOVIE S3. *A. castellanii* infected with *L. pneumophila* Δ*lppA*/pNT28 (72 h post infection, bright field).

MOVIE S4. *A. castellanii* infected with *L. pneumophila* Δ*icmT*/pNT28 (72 h post infection, bright field).

TABLES

TABLE 1. Strains and plasmids.

Strain/plasmid	Relevant properties [a]	Reference
E. coli		
TOP10		Invitrogen
BL21		Novagen
L. pneumophila		
GS3011	*L. pneumophila* JR32 *icmT3011*::Kan^R (Δ*icmT*)	(58)
JR32	Virulent *L. pneumophila* serogroup 1 strain Philadelphia	(59)
RM01	*L. pneumophila* JR32 *lpg2819*::Kan^R (Δ*lppA*)	This work
Plasmids		
pAK7	Expression of N-terminal His-tag fusions, pET-28a(+)-based	This work
pCR33	*Legionella* expression vector, Δ*mobA*, RBS, M45-(Gly)$_5$, Cam^R, (= pMMB207-C-RBS-M45)	(17)
pCR76	pMMB207-C-P$_{tac}$-RBS-*gfp*-RBS-MCS	(25)
pET-28a(+)	Expression of N-terminal His-tag fusions; P$_{T7}$; Kan^R	Novagen
pGEX-6P-1	GST expression vector	GE Lifesciences
pGEX-4T-1	GST expression vector	GE Lifesciences
pGEM-T-easy	Cloning vector	Promega
pLAW344	*L. pneumophila* suicide vector	(60)
pMMB207-C	*Legionella* expression vector, Δ*mobA*, w/o RBS, Cam^R	(46)
pNT28	pMMB207-C-RBS-*gfp* (constitutive *gfp*)	(44)
pPhyA	Synthetic construct of *S. ruminantium phyA* gene	This work
pRM1	pMMB207-C-RBS-M45-*lppA*	This work
pRM2	pGEM-T-easy-*lppA*$_{down}$_Kan^R_*lppA*$_{up}$	This work
pRM3	pLAW-*lppA*$_{down}$_Kan^R_*lppA*$_{up}$	This work
pRM4	pGEX-4T-1-*lppA*	This work
pRM9	pGEX-6P-1-*lppA*$_{Δ1-16}$	This work
pSE7	pGEX-6P-1-*lppA*$_{Δ1-16,}$ C215A	This work
pSE8	pGEX-6P-1-*lppA*$_{Δ1-16,}$ K219A	This work
pSE9	pGEX-6P-1-*lppA*$_{Δ1-16,}$ R221A	This work
pSE10	pGEX-6P-1-*lppA*$_{Δ1-16,}$ G220D	This work
pSH97	pMMB207-C-RBS-*cyaA* (including polylinker)	(25)
pSH100	pMMB207-C-*cyaA*-*ralF*	(25)
pSH108	pMMB207-C-*cyaA*-*lppA*	This work
pSU4	GFP-SidC$_{P4C}$ in pDXA, G418^R	(18)
pSW001	pMMB207-C, Δ*lacI*^{q} (constitutive *dsred*)	(61)
pSW013	pGEX-4T-1-*lpnE*	(23)
pWS11	pET28a(+)-*lppA*$_{21-314}$	This work
pWS25	pGEX-6P-1-*phyA*$_{Δ1-16}$	This work
pWS31	pMMB207-C-RBS-*gfp*-RBS-*lppA*	This work

[a] Abbreviations: Amp, ampicillin; Cam, chloramphenicol; G418, geneticin; Kan, kanamycin

TABLE 2. Oligonucleotides used in this study.

Oligo	Sequence (5' - 3') [a]	Comments
oCR149	GCTGTTGACAATTAATCATCGG	pMMB207 fo (sequencing)
oCR150	CGTTCTGATTTAATCTGTATCAGGC	pMMB207 re (sequencing)
oCR161	AAAAACGCGGATCCATGAGCTTTAAAGGATTTAAAGTG	5' of *lppA*, *Bam*HI
oCR162	AAAAACGCTCTAGACTATTACTAGATATTGAGCTTTTTC CATTC	3' of *lppA*, *Xba*I
oAK7fo	GGACGCTCATGAAAAAAAATCACCACCATCATCACCAC CTAGTTCCGCGTGGATCCGAATGG	*Bsp*HI/*Bam*HI
oAK7re	CCATTCGGATCCACGCGGAACTAGGTGGTGATGATGGTG GTGATTTTTTTTCATGAGCGTCC	*Bam*HI/*Bsp*HI
oKan3'	TCACTTTCTGGCTGGATGATGG	5' out of Kan^R (deletion)
oKan5'	GAATATGGCTCATAACACCCC	3' out of Kan^R (deletion)
oRM1	AAAAACGCGGATCCCATCTAGTGCCATTTGCAAG	5' of *lppA* downstream region (deletion), *Bam*HI
oRM2	TTAGCGATACCTGGAAATAAG	3' of *lppA* downstream region (deletion)
oRM3	GGTCATAACGATGCAAATAGTAG	5' of *lppA* upstream region (deletion)
oRM4	AAAAACGCGGATCCAATAAATCCTTTTTAAATCCCTAAAG ATG	3' of *lppA* upstream region (deletion), *Bam*HI
oRM5	AAAAACGCGGATCCATGAGCTTTAAAGGATTTAAAG	5' of *lppA*, *Bam*HI
oRM6	AAAAACGCGTCGACCTAGATATTGAGCTTTTTCCATTC	3' of *lppA*, *Sal*I
oRM7	GGCTGTCTGATTTTCCTCAAG	3' of *lppA* downstream region
oRM8	CTGCCCGAATGGTATCAG	5' of *lppA* upstream region
oRM13	AAAAACGCGGATCCCAAAGTTATGCCTCTAAATTG	5' of $lppA_{\Delta 1\text{-}16}$, *Bam*HI
oSE7	GGTATCATGTCCACGCCCGTGGCGGGAAAGGC	5' of *lppA* C215A
oSE8	GCCTTTCCCGCCACGGGCGTGGACATGATACC	3' of *lppA* C215A
oSE9	GCCGTGGCGGGGCAGGCCGTACGACG	5' of *lppA* K219A
oSE10	CGTCGTACGGCCTGCCCCGCCACGGC	3' of *lppA* K219A
oSE11	CGTGGCGGGAAAGGCGCTACGACGACTGTTTTTGC	5' of *lppA* R221A
oSE12	GCAAAAACAGTCGTCGTAGCGCCTTTCCCGCCACG	3' of *lppA* R221A
oSE13	CCGTGGCGGGAAAGACCGTACGACGACTG	5' of *lppA* G220D
oSE14	CAGTCGTCGTACGGTCTTTCCCGCCACGG	3' of *lppA* G220D
oWS25	AGTTATGGATCCAAATTGGCATCCTCC	5' of $lppA_{21\text{-}314}$, *Bam*HI (crystallization)
oWS26	CTAGATGTCGACTTATTACCATTCTGACCA	3' of $lppA_{21\text{-}314}$, *Sal*I (crystallization)
oWS73	AAAAAAGGATCCGCCAAGGCGCCGGAGCAGACGGTGAC GG	5' of *phyA*, *Bam*HI

oWS91	AAAAAAGTCGACCTACTTCGCCGGATGGCTCTTGAGCCA G	3' of *phyA*, *Sal*I

[a] Restriction sites are underlined.

TABLE 3. Data collection and refinement statistics for LppA.

Data processing	
Space group	P 1 2_1 1
Cell dimensions *a*, *b*, *c* (Å), β (°)	98.65 55.49 131.42 99.61
Resolution (Å)	50 – 1.4 (1.5 – 1.4)*
R_{meas} (%)	5.4 (82.8)
$I / \sigma I$	15.9 (2.3)
CC(1/2) (%)	99.9 (81.7)
Completeness (%)	96.0 (90.5)
Redundancy	4.5 (4.6)
Refinement	
Resolution (Å)	50.0 – 1.4
No. reflections (Test reflections)	264665 (1060)
R_{work} , R_{free} (%)	14.4 , 16.9
No. atoms	12052
Protein	10529
Ligand/ion	59
Water	1464
***B*-factors (A^2)**	
Protein	23.8
Ligand/ion	19.5
Water	35.6
R.m.s deviations	
Bond lengths (Å)	0.007
Bond angles (°)	1.13
Ramachandran plot (Molprobity)	
Allowed (%)	2.0
Favored (%)	98.0

*Outermost resolution shell

FIGURE 1

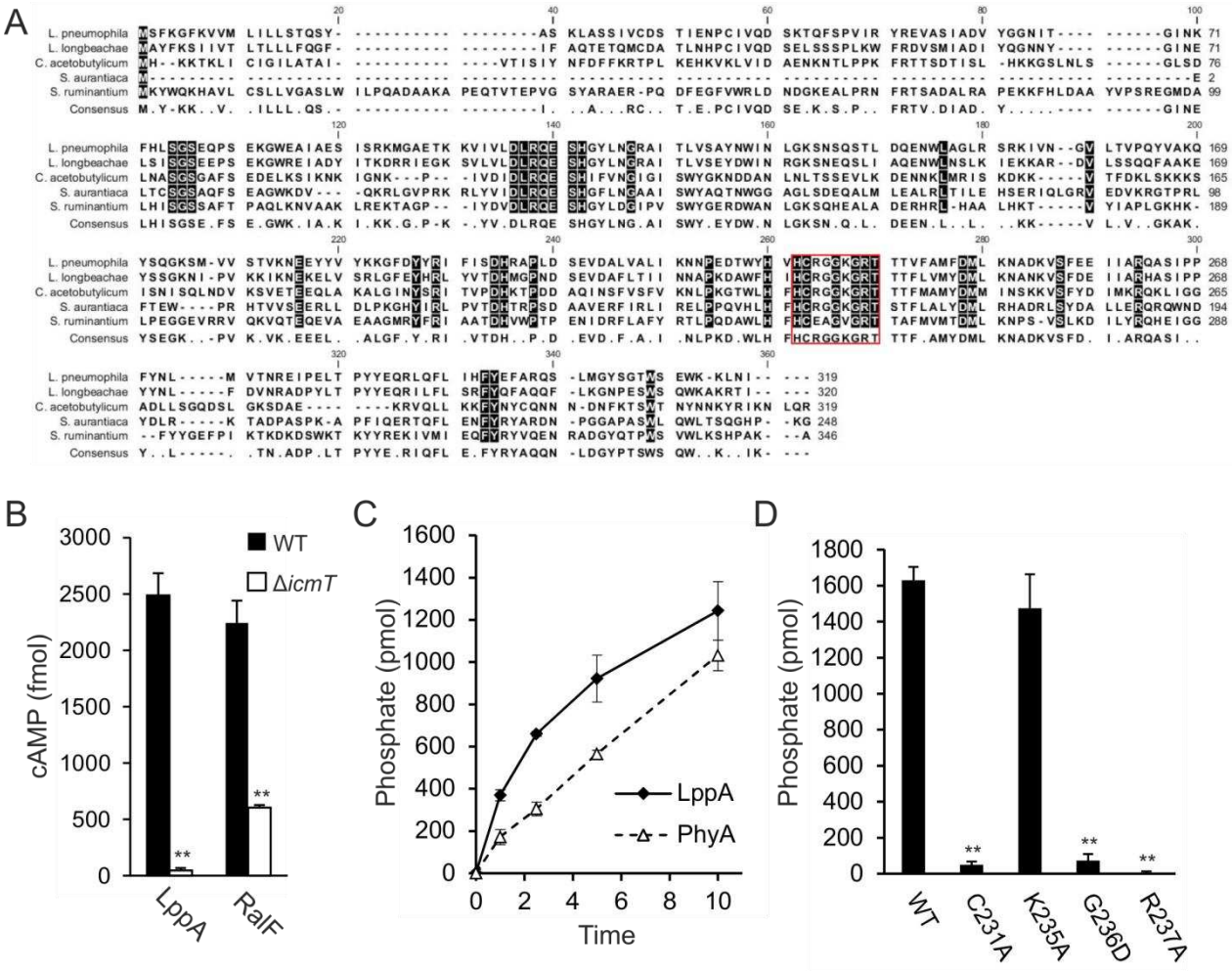

FIGURE 2

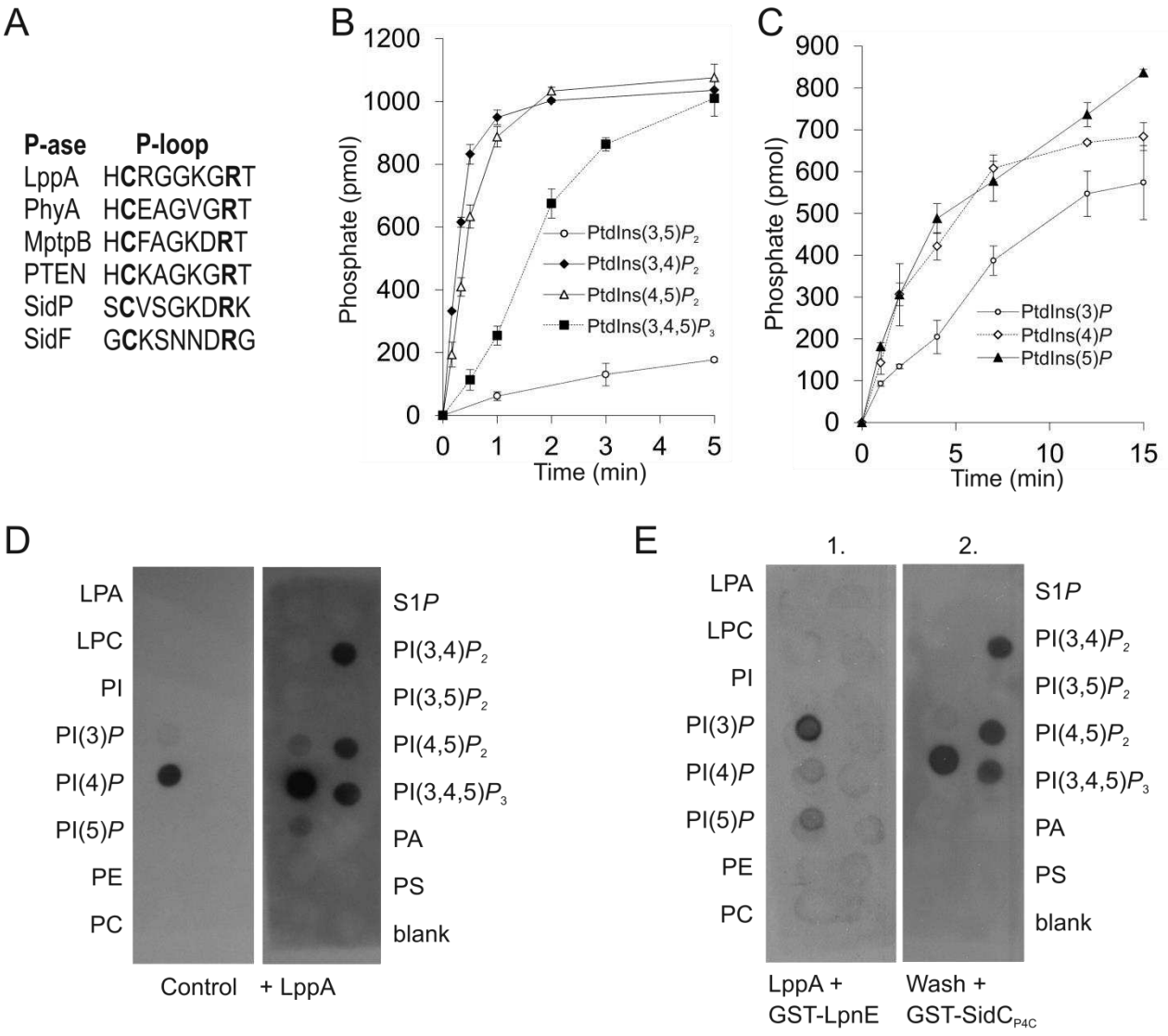

FIGURE 3

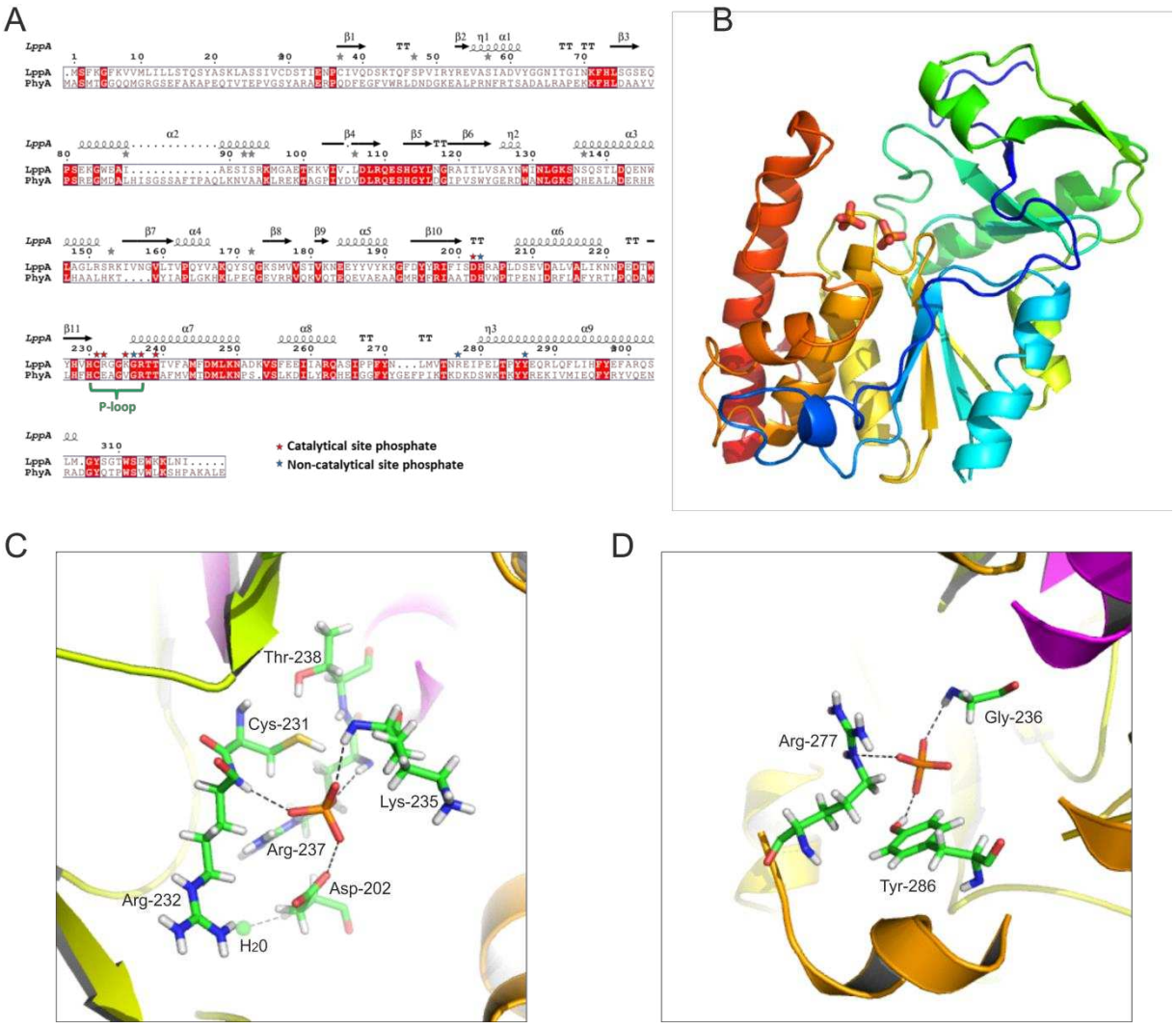

FIGURE 4

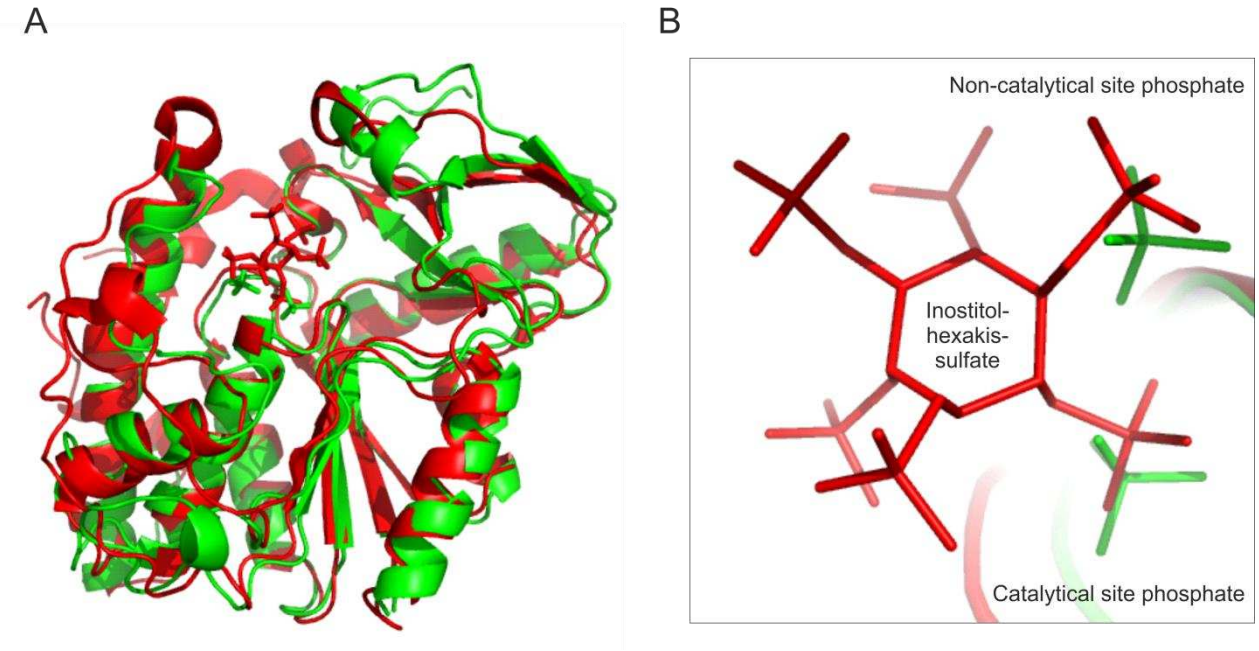

FIGURE 5

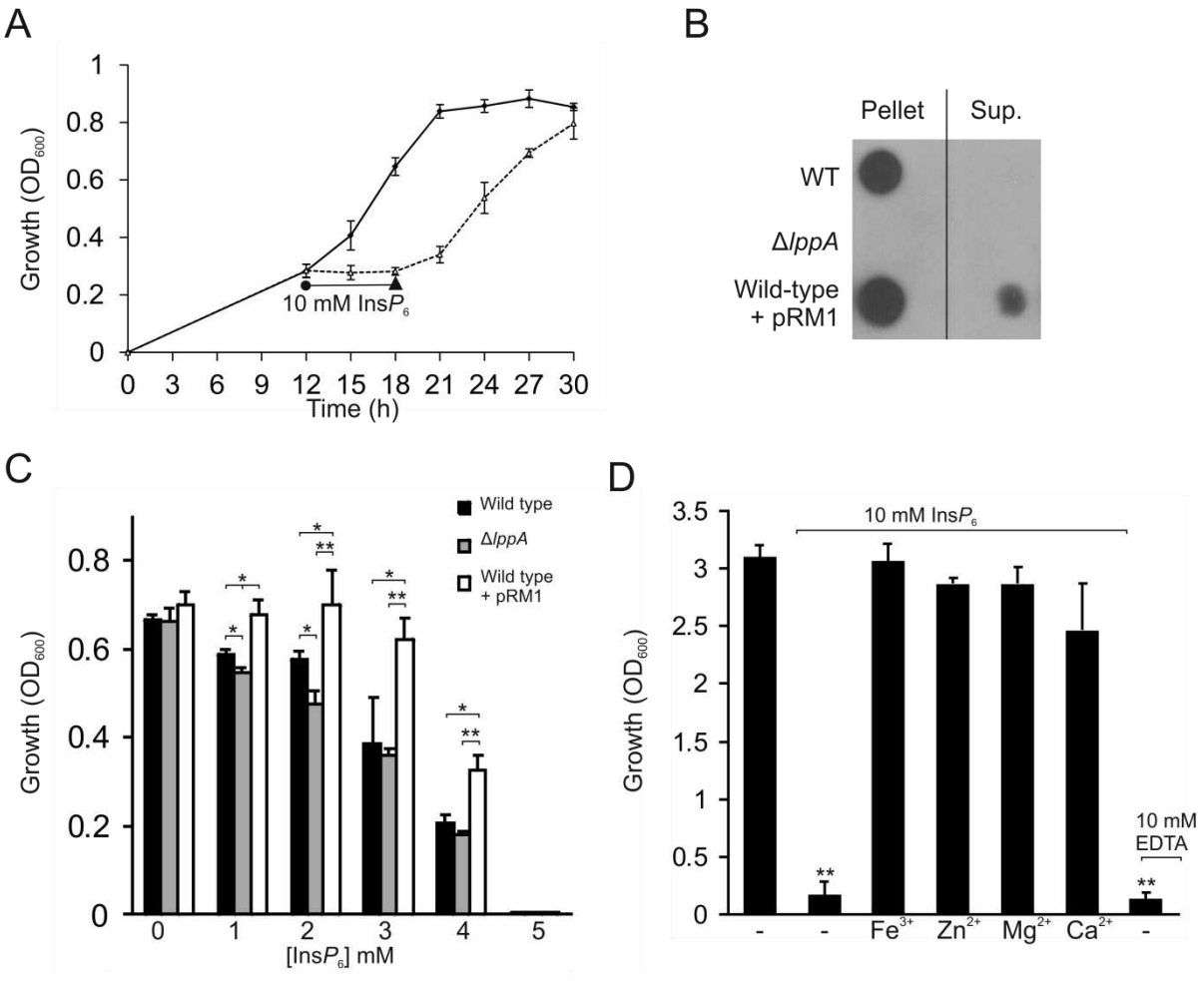

FIGURE 6

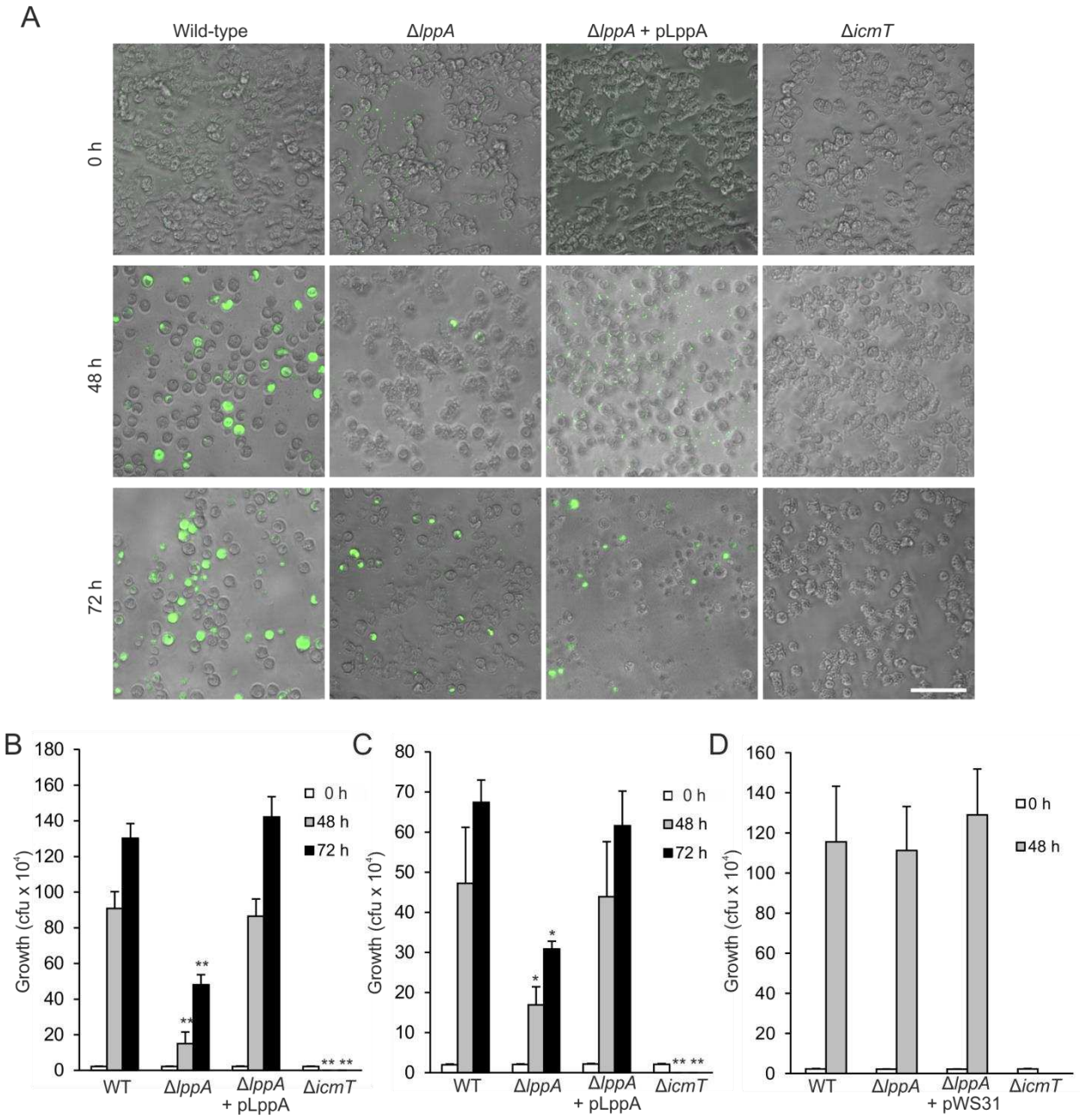

FIGURE 7

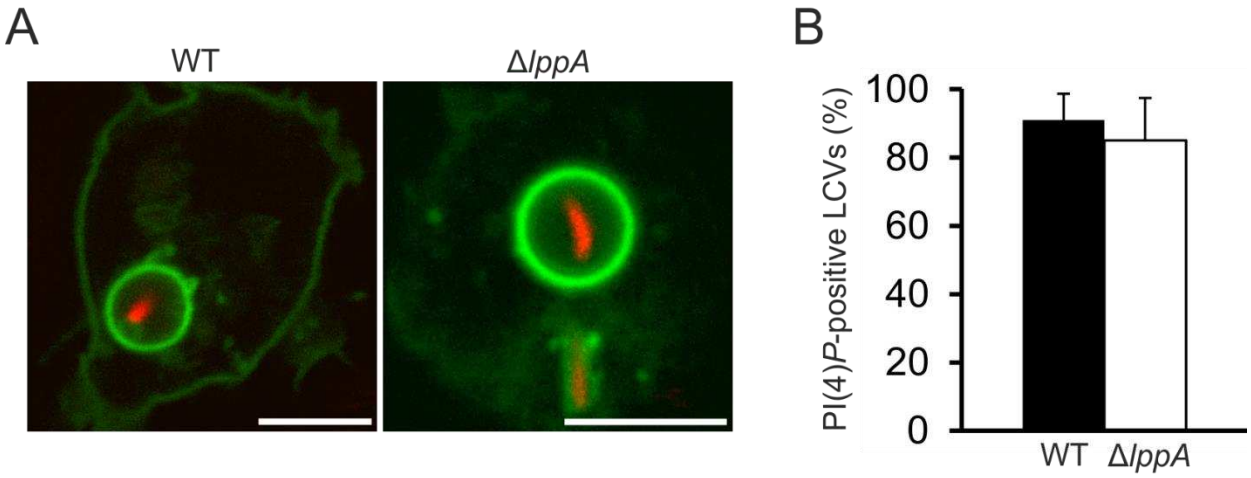

Microbiology:

A Type IV-Translocated Legionella Cysteine Phytase Counteracts Intracellular Growth Restriction by Phytate

Stephen Weber, Christian U. Stirnimann, Mara Wieser, Daniel Frey, Roger Meier, Sabrina Engelhardt, Xiaodan Li, Guido Capitani, Richard A. Kammerer and Hubert Hilbi

J. Biol. Chem. *published online October 22, 2014*

Access the most updated version of this article at doi: 10.1074/jbc.M114.592568

Supplemental material:
http://www.jbc.org/content/suppl/2014/10/22/M114.592568.DC1.html

This article cites 0 references, 0 of which can be accessed free at
http://www.jbc.org/content/early/2014/10/22/jbc.M114.592568.full.html#ref-list-1